CrossMark

ORIGINAL ARTICLE

Preparation, physicochemical characterization and in vitro dissolution studies of azithromycin-cyclodextrin inclusion complexes

Mei-rong Zhao[1] · Li-sheng Wang[1] · Hua-wen Liu[1] · Ya-jing Wang[1] · Hua Yang[1]

Abstract To improve the water solubility of hydroxypropyl-β-cyclodextrin(HP-β-CD, 500–800 mg/mL), a novel hydroxypropyl-β-cyclodextrin polymer (HP-β-CDP) was firstly synthesized and characterized by Fourier Transform Infrared spectroscopy (FT-IR), Nuclear magnetic resonance (^{1}H-NMR), and X-ray diffraction spectroscopy (XRD) comprehensively. The solubility of HP-β-CDP was determined as 40.2 g/mL, which is about 46.6 times more than HP-β-CD. The inclusion complexes were prepared with HP-β-CD and HP-β-CDP by saturated solution method to improve the solubility and in vitro release behavior of insoluble drug AZM. The formulation was optimized by orthogonal design with three factors and three levels L_9 (3^4). Solubility, FT-IR, XRD and scanning electron microscope investigations demonstrated that both HP-β-CD and HP-β-CDP effectively formed the inclusion complex. The resultant HP-β-CDP complex presented an increased AZM solubility (628.5 ± 0.25 μg/mL) than HP-β-CD (311.3 ± 0.26 μg/mL) compared with AZM (34.2 ± 0.30 μg/mL) in water. The in vitro accumulative release studies revealed that more than 90 % of AZM could be released from HP-β-CDP inclusion complex within 1 h, which is far more than free AZM (27.5 %) and HP-β-CD inclusion complex (46.5 %). The studies indicated that HP-β-CDP with better water solubility could improve remarkably the solubility and release properties of AZM than HP-β-CD.

Keywords HP-β-CD · Inclusion complex · Solubilization · Dissolution · Release kinetic models

Introduction

Azithromycin (AZM), as the first azalide antibiotic with a methyl-substituted nitrogen atom incorporated into the 15-membered lactone ring (Fig. 1a), is a subclass of macrolide antibiotics. It is widely used for the treatment of bacterial infections as it has many advantages, such as a wide antibacterial spectrum, long half-life, high tissue permeability and fewer side effects. So far, the market available formulations including tablets, capsules, granules, dispersible tablets, dry suspensions [1, 2], enteric-coated capsules [3] and injections forms, have been developed to enhance the solubility and stability of AZM [4, 5].

Cyclodextrins (CD) are nontoxic cyclic oligosaccharides derived from starch, which can form water-soluble inclusion complexes with small molecules and portions of large compounds. β-Cyclodextrins (β-CD) are important materials in drug delivery systems since they can function as host for both polar and nonpolar guests [6]. β-CD can modify the physical, chemical and biological properties of drug molecules through the formation of inclusion complexes. The stability, solubility and bioavailability of drugs can be increased, the taste can be shielded and tissue irritation of drugs can be decreased [7–10]. However, the practical application of β-CD in drug delivery is restricted by its low solubility in aqueous solution (18.5 mg/mL), the potential formation of crystalline complexes and so on.

✉ Ya-jing Wang
  wangyjing@gmail.com

✉ Hua Yang
  yanghua6316@sina.com

[1] Pharmacy Engineering Specialty, College of Chemistry and Chemical Engineering, GuangXi University, 100, Daxue Road, Nanning 530004, Guangxi, China

Fig. 1 Chemical structure of HP-β-CD (**a**) and AZM (**b**), the synthesis of HP-β-CDP (**c**)
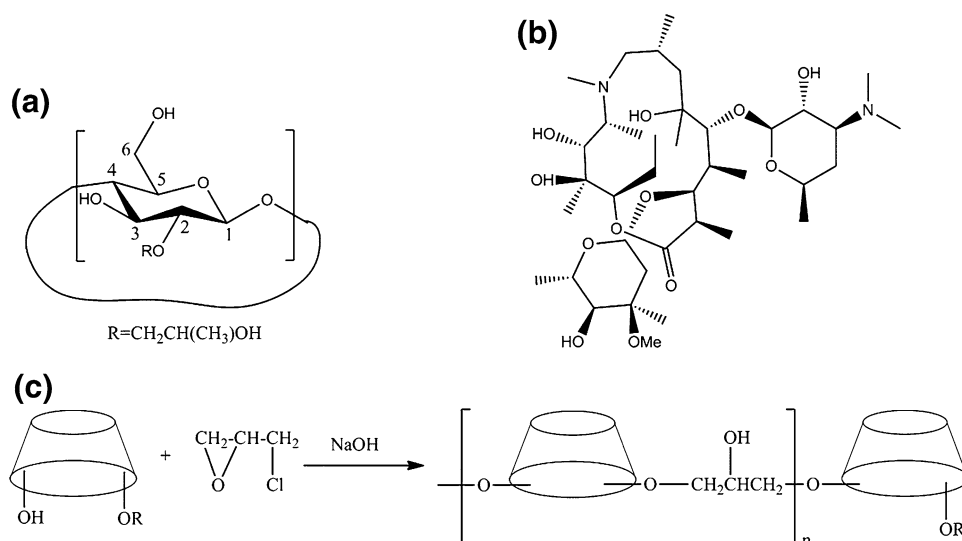
Various kinds of β-CD derivatives have been prepared to improve the physicochemical properties of the parent β-CD as multi-functional drug carriers [11–14], such as hydroxypropyl-β-CD (HP-β-CD) (Fig. 1b) [15, 16]. Beside the utilization of β-CD monomers, the polymers have also been developed [8, 9, 17, 18]. The polymeric form was supposed to increase the stability constant of these complexes.

In the present study, we developed a facile way to prepare a highly hydrophilic HP-β-CD polymer (HP-β-CDP), which is supposed to possess a bigger hydrophobic cavity and stability constant. The structure of HP-β-CDP was fully characterized by Fourier transform infrared spectroscopy (FT-IR), nuclear magnetic resonance (^{1}H-NMR), and X-ray diffraction spectroscopy (XRD). The solubility of HP-β-CDP was determined and compared with that of HP-β-CD. The inclusion complexes were prepared by saturated solution method with HP-β-CD and HP-β-CDP respectively, and the formulations were optimized by orthogonal design. The in vitro accumulative release profiles of resultant HP-β-CD and HP-β-CDP complex were compared and simulated by model dependent method to explore the differences of release mechanism. The studies indicated the potential of HP-β-CDP to be employed as insoluble drug carrier to improve the solubility and release behavior of insoluble drugs.

Materials and methods

Materials

AZM (F_W = 749, Purity > 99 %), Hydroxypropyl-β-cyclodextrin (HP-β-CD, F_W = 1330, Purity > 99 %) were purchased from the HuBei Prosperity Galaxy Chemical Co., Ltd. Epichlorohydrin (EP, A.R., Tianjin Damao Chemical Reagent Factory, China). Other reagents and chemicals were of analytical reagent grade and used without further purification. Distilled water was used throughout the experiment.

Preparation of the HP-β-CD polymers(HP-β-CDP) [19, 20]

Water soluble HP-β-CDP was prepared by crosslinking HP-β-CD with EP under strongly alkaline conditions (NaOH 30 %, w/v) with molar ratio 1:16. The reaction was stopped at the immediate vicinity of gelation for 4 h by adding a small amount of acetone. HP-β-CDP was obtained after shaking off acetone at 56 °C followed by cooling to room temperature (R.T., 25 ± 1 °C). The reaction solution was adjusted by 3 mol/L HCl to neutral. The details of the synthesis and purification are described elsewhere [20]. The products were further purified by dialysis tubing with a molecular weight cut off 8000–14,000 to remove the remained salt and unreacted composition. The purified products were verified by the addition of AgNO$_3$ [21], and no chloride reaction would be observed. The synthesis route is shown in Fig. 2.

Characterization of the HP-β-CDP

FT-IR

Infrared spectra of HP-β-CDP was recorded with infrared spectrophotometer(FTIR-8400S, SHIMADZU, JAPAN) by mixing and compressing a small amount of HP-β-CDP
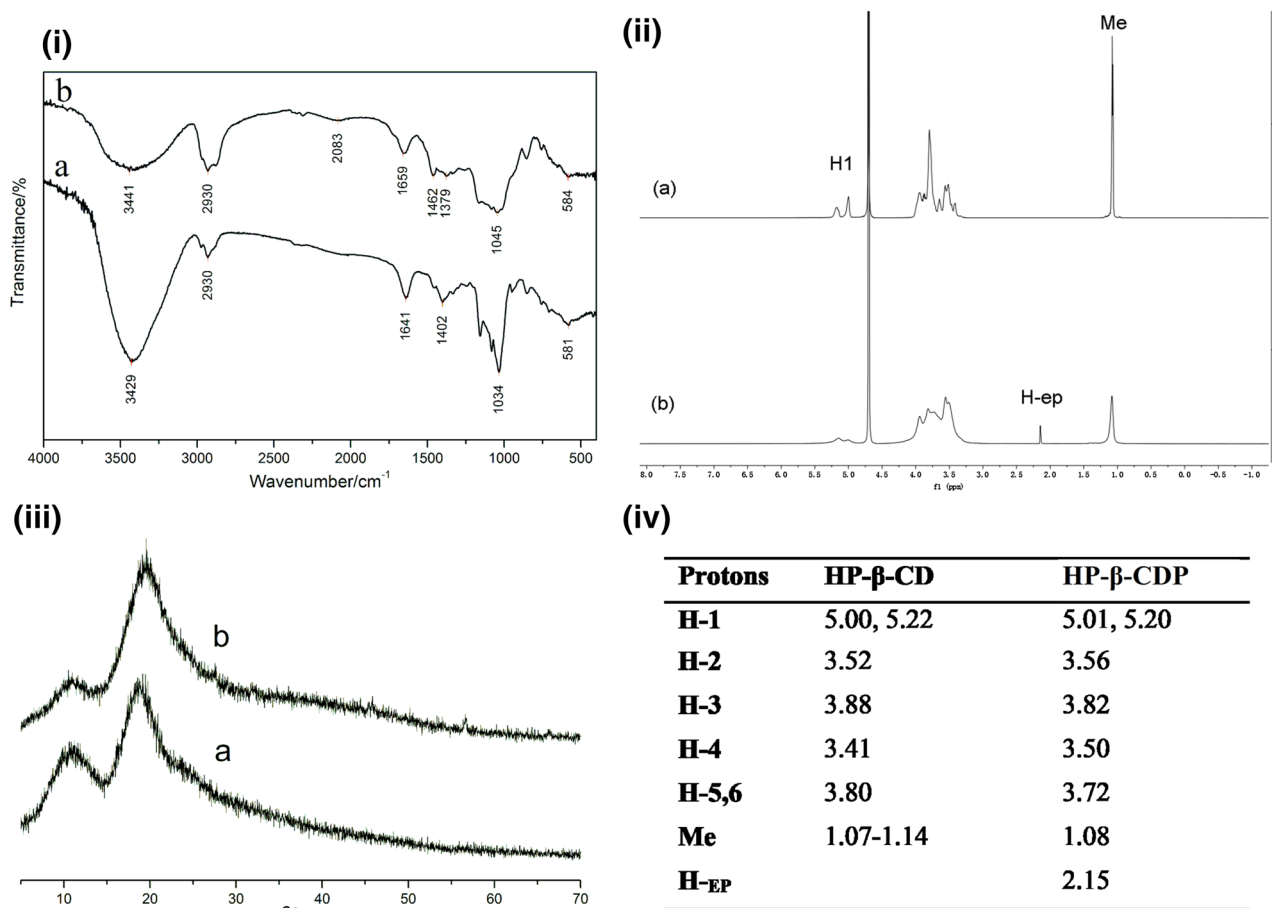
Fig. 2 (**i**) FT-IR spectra of HP-β-CD (*a*) and HP-β-CDP (*b*), (**ii**) The ^{1}H-NMR of HP-β-CD (*a*) and HP-β-CDP (*b*), (**iii**) X-ray diffraction spectra of HP-β-CD (*a*) and HP-β-CDP (*b*), (**iv**) Chemical shift (δ) of HP-β-CD and HP-β-CDP

with KBr using a manual hydraulic press. The spectra were recorded over the range of 4000–400 cm^{-1}.

^{1}H-NMR

^{1}H-NMR is the most effective method to clarify the formation of HP-β-CDP. The ^{1}H-NMR spectra of HP-β-CD and HP-β-CDP in 99.98 % D$_2$O were recorded with NMR spectrometer (Ascend 600 MHz NMR Spectrometer (AVANCEIII HD600MHZ, BRUKER, SWITZERLAND)) at 25 °C.

XRD

XRD patterns were obtained with Cu-Kα radiation (40 kV, 100 mA) at a scanning rate of 10°/min (D/MAX-3B DIFFRACTOMETER, RIGAKU, JAPAN). Powder samples were mounted on a vitreous sample holder and scanned with a step size of 2θ = 0.02° for 2θ values between 5 and 70°.

Preparation of inclusion complex

Standard curve of AZM

Accurately weighed an amount of AZM, preparing for a certain concentration of a solution in pH 6.0 phosphate buffer with and without sulfuric acid adding, corresponding reagent blank at 190-600 nm of the UV spectra were scanned [22]. By comparing with the maximum absorption wavelength, 482 nm was selected for detection by UV spectrometer.

Preparation of AZM inclusion complex [21]

AZM inclusion complex was prepared by saturated solution method with HP-β-CD and HP-β-CDP, respectively. Briefly, the HP-β-CD and HP-β-CDP were weighed precisely and dissolved in water to obtain super saturated solution, while 0.2 g AZM was dissolved in a small amount of ethanol. The AZM in ethanol solution was gently added into the HP-β-CD and HP-β-CDP super solution and stirred at 40 °C for 3 h to obtain milky solutions. The product was

cooled at 4 °C for 24 h and filtrated by 40 μm filter. The filtrate was washed by absolute ethanol to remove the residual AZM and dried under vacuum at 45 °C for 24 h. The product was stored in desiccator and named as AZM-HP-β-CD and AZM-HP-β-CDP respectively for further use. Inclusion ratio is calculated as the Eq. (1)

$$\text{Inclusion ration(EE, \%)} = \frac{\text{the amount of drug in clathrate}}{\text{added in an amount of drug}} \times 100\%$$

(1)

The formulation was optimized by univariate analysis and orthogonal experiment design. The effects of molar ratio of HP-β-CD/AZM and mass ratio of HP-β-CDP/AZM, inclusion temperature and time on the inclusion ratio were evaluated.

The physical mixtures of AZM with HP-β-CD (1:1, molar ratio) and HP-β-CDP (1:20, mass ratio) were prepared by thoroughly mixing the two components in a Ceramic mortar for 10 min. The obtained products were collected and named AZM&HP-β-CD and AZM&HP-β-CDP respectively.

Characterization of Inclusion complex

UV spectra

UV spectra were recorded for AZM, HP-β-CD, HP-β-CDP, AZM&HP-β-CD and AZM&HP-β-CDP, AZM-HP-β-CD and AZM-HP-β-CDP in pH = 6.0 phosphate buffer with sulfuric acid added. The samples were stayed half an hour at R.T and then scanned in the wavelength range from 200 to 600 nm. The spectral bandwidth used was 0.1 nm and the scanning interval was 1 nm.

FT-IR

The FT-IR spectra of AZM, HP-β-CD, HP-β-CDP, AZM&HP-β-CD and AZM&HP-β-CDP, AZM-HP-β-CD and AZM-HP-β-CDP were recorded between 4000 and 400 cm^{-1}. The sample preparation was described in item "FT-IR".

XRD

The XRD patterns were obtained at a scanning rate of 10°/min with Cu-Kα radiation (20 kV, 5 mA). Powder samples were mounted on a vitreous sample holder and scanned with a step size of 2θ = 0.02° between 2θ = 5° and 50°.

Scanning electron micrographs (SEM)

SEM is a qualitative method to observe the surface morphology of the substance. The SEM of products were obtained with the environmental scanning electron microscope (QUANTA 200, FEI, USA). The samples were evenly distributed on SEM specimen stubs with double adhesive tape and the micrographs were obtained with an accelerating potential of 20 kV under vacuum.

Solubility studies of AZM-HP-β-CD and AZM-HP-β-CDP [23–25]

Solubility studies were carried out according to the method reported. In brief, excess amounts of AZM or inclusion complexes prepared with the HP-β-CD and HP-β-CDP according to the method described in "Preparation of AZM inclusion complex [21]" section were added into 10 mL of water, then the suspensions were stirred continuously at R.T. for 48 h until equilibrium was attained. Supersaturated solutions were filtered through a 0.45 μm Millipore filter. The AZM concentrations were measured at 482 nm after properly diluted by sulfuric acid and cooled for 30 min. The corresponding HP-β-CD and HP-β-CDP were used as blank controls for inclusion complexes. All the experiments were repeated for 3 times and expressed as mean ± SD (n = 3).

Dissolution studies [26, 27]

The dissolution behaviors of the resultant complexes were carried out in Intelligent Dissolution Tester (ZRS-8LD, Tianda Tianfa, China) at 100 rpm and 37 °C. Powder samples of AZM, its physical mixtures and inclusion complexes containing 20 mg of AZM were sealed with three layers Gauze and placed into stainless steel baskets with 250 mL of pH = 6.8 phosphate buffer solution as dissolution media. At pre-specified time points(5, 10, 15, 30, 45, 60, 90, 120, 150, 180 min), the samples (5 mL) were withdrawn from dissolution media and filtered by 0.45 μm Millipore filter, meantime, 5 mL pH = 6.8 phosphate buffer solution was supplemented to the dissolution media. The concentration of AZM was determined at 482 nm.

Results

Synthesis and characterization of the HP-β-CDP

FT-IR analysis of HP-β-CDP

FT-IR was generally used to confirm the formation of HP-β-CDP by investigating the variation of peak shape, shift and intensity [5, 10, 28]. As seen in Fig. 2(i), the HP-β-CDP still retains HP-β-CD original empty cavity structure. The absorption bands of HP-β-CDP in Fig. 2(i) b at 1659, 1462,

and 1045 cm^{-1} were assigned to H–O–H bending, CH$_2$ bending and asymmetric C–O–C stretching vibration respectively. More importantly, a broad band at around 3441 cm^{-1} represented the symmetric and asymmetric O–H stretching vibration due to the many intermolecular hydrogen bonds of HP-β-CDP, and another bond at 2930 cm^{-1} was assigned to CH$_2$ antisymmetric stretching vibration. Besides, the absence of the characteristic peaks of the crosslinking agent (EP) at 1250 cm^{-1} (epoxy ring) and 1270 cm^{-1} (C–Cl) indicated that all the EP was reacted.

^{1}H-NMR analysis

The ^{1}H-NMR of HP-β-CD and HP-β-CDP were presented in Fig. 2(ii). In the spectrum of HP-β-CD, the signal for H-1, H-2, H-3, H-4, H-5 and H-6 located at 5.00–5.20, 3.52, 3.88, 3.41 and 3.80, respectively, as seen in Fig. 2(iv), were corresponding to the previous literatures [29–32]. The two broad signals for H-1 centered at 5.00 and 5.20 ppm was due to the different types of anomeric protons [33]. In the spectrum for HP-β-CDP, appreciable chemical shift changes were observed with respect to the spectra for the HP-β-CD. From Fig. 2(iv) we could see the signals of H-1, H-2 and H-4 protons on the outer surface of HP-β-CD changed with positive Δ δ values of 0.01, 0.04 and 0.09 respectively. While upper Δ δ shift values of 0.08 by H-5 protons in the inner surface of HP-β-CD were recorded, and Δ δ for H-3(0.06, near the wide side of the cavity) was smaller than H-5(0.08, near the narrow side). More obviously, the triplet peak (δ 1.07–1.14) assigned to the CH$_3$CHOHCH$_2$ - of the HP-β-CD changed to single peak (δ 1.08), and a new peak (δ 2.15) from proton specifically on the EP located on the HP-β-CDP appeared. We can propose from the ^{1}H-NMR data that HP-β-CDP was obtained.

X-ray powder diffraction spectra (XRD) analysis

The powder XRD patterns of HP-β-CD and HP-β-CDP was shown in Fig. 2(iii). The XRD pattern of HP-β-CD shows two wide band at approximately at 2θ = 11.22° and 19.14° respectively, thus confirming the amorphous nature of HP-β-CD. Our results are in agreement with former researchers [29, 31, 32]. While the resultant HP-β-CDP exhibits similar two wide band at 2θ = 10.52° and 19.56°, indicating amorphous HP-β-CDP retains HP-β-CD original empty cavity. Besides, it was noticed that the intensity of band at 2θ = 10.52° decreased, probably resulting from the crosslinked structure of HP-β-CDP.

Standard curve of AZM

The AZM assay was determined by a simple, accurate and rapid spectrophotometric method. AZM was hydrolyzed with sulfuric acid firstly and the maximum absorbance was shifted from 205 to 482 nm, as shown in Fig. 3(i). The absorbance of a series of AZM solutions was recorded at 482 nm at 25 °C. The standard curve was obtained by plot absorbance (A) versus AZM concentrations (C, μg/mL), which could be depicted by the equation: $A = 0.007C + 0.035$ ($\gamma^2 = 0.9993$).

Formulation optimization

The effects of molar ratio of HP-β-CD/AZM (mass ratio of HP-β-CDP/AZM), inclusion temperature and time on the inclusion ratio were evaluated by univariate analysis.

Effect of molar/mass ratio on inclusion ratio

As shown in Fig. 4a, d, the inclusion ratio of AZM-HP-β-CD and AZM-HP-β-CDP increased with the increase in molar/mass ratio of excipient versus AZM firstly. Inclusion ratio of AZM-HP-β-CD and AZM-HP-β-CDP reached the maximum of 47.2 and 63.7 % with molar/mass ratio of excipient versus AZM at 1:1 and 20:1, respectively. More interestingly, inclusion ratio of AZM-HP-β-CDP decreased, compared with negligible change of inclusion ratio of AZM-HP-β-CD with the continuing increase of molar/mass ration of excipient versus AZM. The results suggested that inclusion ratio of HP-β-CDP depends on its hydrophobic cavity and high solubility in water.

Effect of inclusion temperature on inclusion ratio

As shown in Fig. 4b, e, the inclusion ratio of inclusion complex presented a similar way with the temperature increasing for both of AZM-HP-β-CD and AZM-HP-β-CDP, which increased to the maximum of 52.4 and 55.7 % when the temperature rose to 40 °C. However, the inclusion ratios declined when the temperature was over 40 °C. The similar results were also found by some authors [17] before who observed that higher temperature did not accelerate the reaction but even an inhibition. Therefore, the optimal temperature was determined as 40 °C.

Effect of inclusion time on inclusion ratio

As shown in Fig. 4c, f, the inclusion ratio of inclusion complex reached maximum 47.5 and 66.3 % for AZM-HP-β-CD and AZM-HP-β-CDP respectively, when the reaction time was prolonged to 3 h. This result was in good accordance with the authors [34] who found that long reaction time did not contribute to inclusion ratio proportionally, on the contrary, too long reaction time would make AZM divorce from inclusion complex.
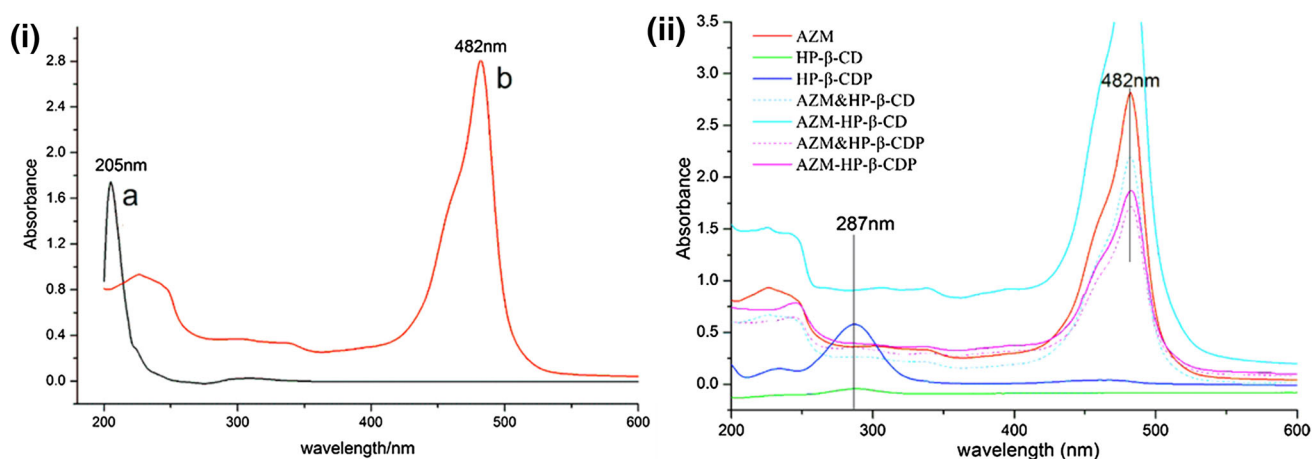
Fig. 3 (**i**) UV Scanning Spectra of AZM (*a*) and AZM colored with sulfuric acid (*b*), (**ii**) UV scanning spectra of AZM, HP-β-CD, HP-β-CDP, physical mixture and inclusion complex
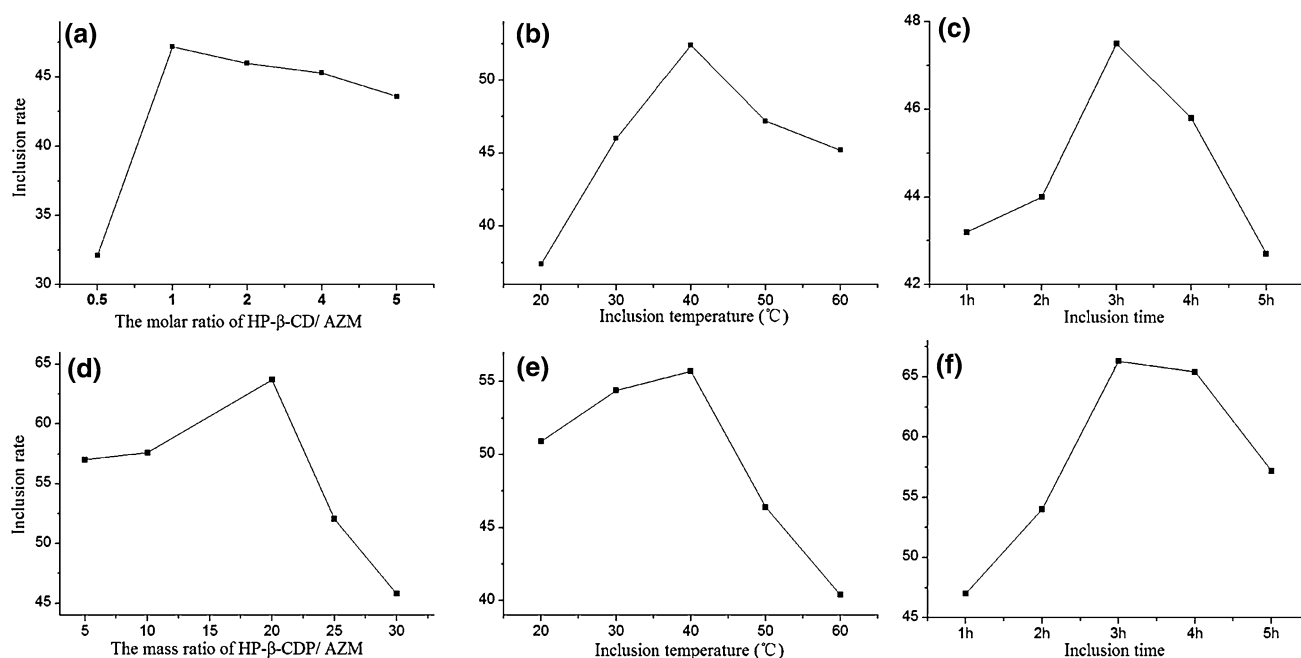

Fig. 4 Effect of reaction parameters on inclusion ratio of HP-β-CD (**a**, **b**, **c**) and HP-β-CDP (**d**, **e**, **f**)

Design and analysis of orthogonal experiment

On the basis of univariate analysis, a L_9 (3^4) orthogonal experiment design was applied to establish the optimum preparation conditions [35, 36]. Inclusion ratio was also set as dependent variable. Three key dependent factors namely mass ratio of HP-β-CDP versus AZM (A), inclusion temperature (B) and inclusion time(C) were studied at three levels, as shown in Table 1. Table 2 provides a brief overview of the orthogonal design and results. By extreme difference analysis(R) it can be concluded that (Table 3), the effects of various factors on the inclusion ratio followed by the order: A > C > B. After rigorous optimization of experimental conditions, the optimum conditions($A_2B_1C_2$) for the inclusion process, namely the mass ratio of HP-β-CDP/AZM 20:1, inclusion time 3 h, inclusion temperature 30 °C were found. These conditions were engaged to generate AZM-HP-β-CDP with inclusion rate up to 72.5 %.

The result of verification

Parallel experiments were carried out for five times to prepare AZM-HP-β-CDP based on the optimum formulation, the inclusion ratio of AZM was determined as

Table 1 Orthogonal design factors and levels

Levels	Factors		
	Mass ratio	Inclusion temperature(°C)	Inclusion time(h)
1	15:1	30	2
2	20:1	40	3
3	25:1	50	4

Table 2 L_9 (3^4) Orthogonal design table and results

No.	A	B	C	Inclusion rate (%)
1	1	1	1	65.0
2	1	2	2	67.0
3	1	3	3	71.1
4	2	1	2	72.5
5	2	2	3	58.8
6	2	3	1	59.3
7	3	1	3	64.6
8	3	2	1	70.9
9	3	3	2	65.4
K_1	67.7	67.3	63.1	
K_2	68.5	65.6	68.3	
K_3	67.0	65.3	64.8	
R	4.17	2.07	3.50	

72.5 ± 0.416 %(n = 5), which verified the optimum conditions are stable and reliable.

Characterization of inclusion complex

UV–Vis spectral comparative analysis

The absorption spectra of AZM, HP-β-CD, HP-β-CDP, their physical mixture, and the inclusion complex are shown in Fig. 3(ii). The results showed that both of HP-β-CD and HP-β-CDP had no absorption at 482 nm but absorption at 287 nm, which indicated that AZM assay could be conducted at 482 nm without the inference from

excipients by UV. We noticed that both AZM&HP-β-CD and AZM-HP-β-CD exhibits similar spectra with the absorption at 287 nm weakened, and the absorbance of inclusion complex was slightly higher than the physical mixture. As for AZM&HP-β-CDP and AZM-HP-β-CDP, the same tendency was observed. The results suggested that UV–Vis spectra may serve as a supplemental tool for the characterization of HP-β-CD based inclusion complex. More studies are needed to further illustrate the interactions between drug and excipients under different treatments.

FT-IR analysis

The FT-IR spectra of AZM, HP-β-CD, HP-β-CDP, their physical mixture, and their inclusion complex are shown in Fig. 5(i). The IR spectra of AZM (a) is characterized by the prominent band at 3495 cm^{-1} for the O–H stretching vibrations and 2970 cm^{-1} for the C-H stretching vibrations, There was a very strong absorption band at 1720 cm^{-1} for C=O stretching vibration, as well as by the 1230, 1188 and 1051 cm^{-1} bands for C–O–C, C–H and C–O stretching vibrations. Meanwhile, the FT-IR spectrum of HP-β-CD (b) is characterized by several peaks. The absorption band of O–H was found at 3429 cm^{-1}. The three sharp absorption peaks at 1402, 1558, 1641 cm^{-1} were ascribed to the characteristic peaks of benzene ring. The FT-IR spectrum of HP-β-CDP (e) is quite similar to HP-β-CD, as resulting from the same parent structure, except the medium bond at 2930 cm^{-1} assigned to CH_2 antisymmetric stretching vibration.

The spectra of the physical mixtures of both AZM&HP-β-CD (c) and AZM&HP-β-CDP (f) corresponded with the superposition of the spectra of the individual components. Interestingly, the spectra of the AZM-HP-β-CD inclusion complex (d) are quiet similar to that of physical mixture, but all peaks shifted to the red direction. As for the spectra of the AZM-HP-β-CDP inclusion complex (g), in comparison with physical mixture (f), the absorption band at 1720 cm^{-1} for C=O stretching vibration from AZM disappeared, which may suggest that stronger interactions existed between AZM and HP-β-CDP.

Table 3 Anova analysis results

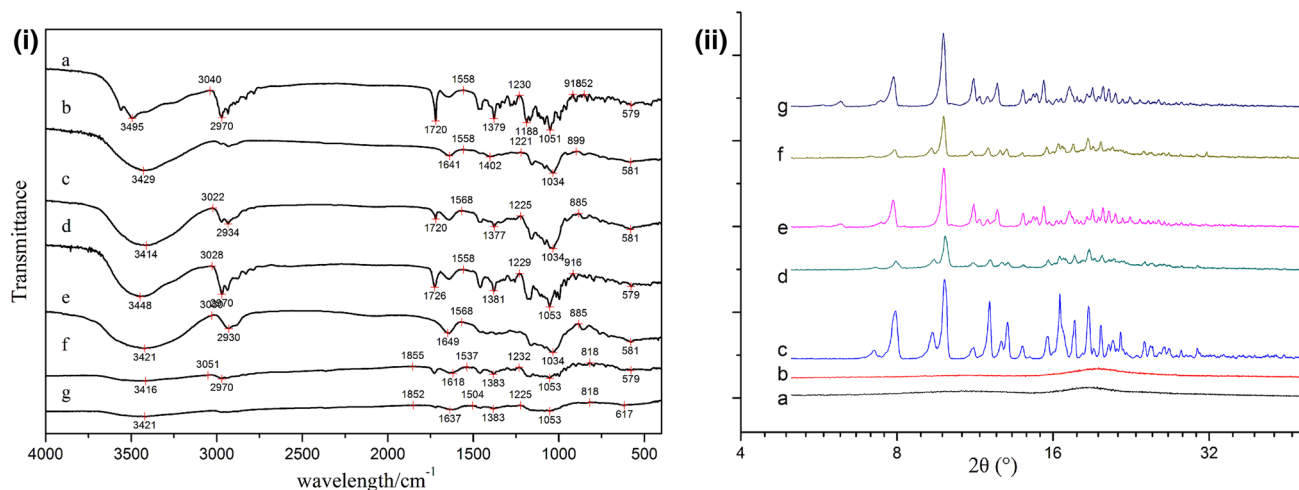| Sources of variance	Deviation from the mean of squares	Freedom	F-value	F-crit
A	29.7	2	1.489	5.14
B	7.53	2	0.377	
C	22.6	2	1.134	
	59.9	6		

注：F_α (2,6) = 5.14, α = 0.05

Fig. 5 (**i**) FT-IR spectra of *a* AZM, *b* HP-β-CD, *c* AZM&HP-β-CD, *d* AZM-HP-β-CD, *e* HP-β-CDP, *f* AZM&HP-β-CDP, *g* AZM-HP-β-CDP; (**ii**) Power X-ray diffraction patterns of *a* HP-β-CD, *b* HP-β-CDP, *c* AZM, *d* AZM&HP-β-CD, *e* AZM-HP-β-CD, *f* AZM&HP-β-CDP, *g* AZM-HP-β-CDP

Powder X-ray diffraction analysis

Powder XRD is a powerful tool to observe the microstructures of crystals and amorphous materials. Generally if the drug (with crystal nature) was encapsulated within the cavity of host molecule (with amorphous nature) [37, 38], the inclusion complexes usually exhibit weakened diffraction peak compared with the parent drug. As shown in Fig. 5(ii), the diffraction pattern of HP-β-CD (a) and HP-β-CDP (b) show two similar wide band with 2θ values near to 10.5° and 19.6°, while AZM(c) exhibits characteristic crystal peaks with 2θ values at 9.86°, 13.08°, 13.18°, 14.78°, 16.5°, 21.58°, 22.8°, 23.98°, 28° and 30.36° respectively. As expected, the characteristic peaks of AZM are present in the diffraction pattern of physical mixtures (d, f) with the similar positions and relative intensity, which indicated that no detectable interactions existed between AZM&HP-β-CD and AZM&HP-β-CDP. In contrast, the XRD pattern AZM-HP-β-CD and AZM-HP-β-CDP inclusion complexes (e, g) are different from that of pure AZM, HP-β-CD, HP-β-CDP and their physical mixtures. Some typical diffraction peaks reduced or disappeared such as at the 2θ values of 7.2°, 9.36°, 12.08°, while some new peaks such as at 2θ values = 6.24° for both of inclusion complexes appeared. This difference may due to inclusion of the AZM molecule into the cavity of HP-β-CD.

SEM analysis

SEM is a qualitative method used to visualize the surface structure of raw materials or the prepared products, i.e., CDs and drugs or the products obtained by different methods, such as physical mixing, solution complexation, coevaporation and others [28, 29]. As shown in Fig. 6, pure

AZM (a) crystalizes in a cubic columnar form with medium dimensions. HP-β-CD (b) existed in spherical particles with cavity structures (b), and the HP-β-CDP (e) appeared in the form of irregular blocky particles, which confirmed the formation of the HP-β-CDP in some way. The SEM photographs of AZM&HP-β-CD (c) revealed some similarities with the crystals of both AZM and HP-β-CD. However, the AZM-HP-β-CD (d) appeared as a compact and homogeneous plate-like structure crystal, which indicated the formation of inclusion complex between HP-β-CD and AZM. Surprisingly, both of AZM&HP-β-CDP (f) and AZM-HP-β-CDP (g) presented as homogenous and amorphous state in the SEM photographs, no visible differences could be found compared with HP-β-CDP(e), which may result from the super-amorphous nature of HP-β-CDP.

Comparative analysis of HP-β-CD, HP-β-CDP solubilization efficiencies towards AZM

The solubility of HP-β-CDP was determined as 40.2 g/mL, which is about 46.6 times more than HP-β-CD (0.863 g/mL), the results indicated that the solubility of resultant HP-β-CDP improved a lot than parent monomer HP-β-CD. The water solubility of AZM in complex inclusion at 25 °C, compared to that of native AZM (34.2 ± 0.30 µg/mL), was remarkably increased to approximately 311.3 ± 0.26 µg/mL (9.1 fold) and 628.5 ± 0.25 µg/mL (18.4 fold) by the solubilizing effects of HP-β-CD and HP-β-CDP respectively. The results showed that HP-β-CDP was more efficient than natural HP-β-CD to solubilize insoluble drug AZM by inclusion complex, which is probably due to the larger empty cavity of HP-β-CDP after polymerization.
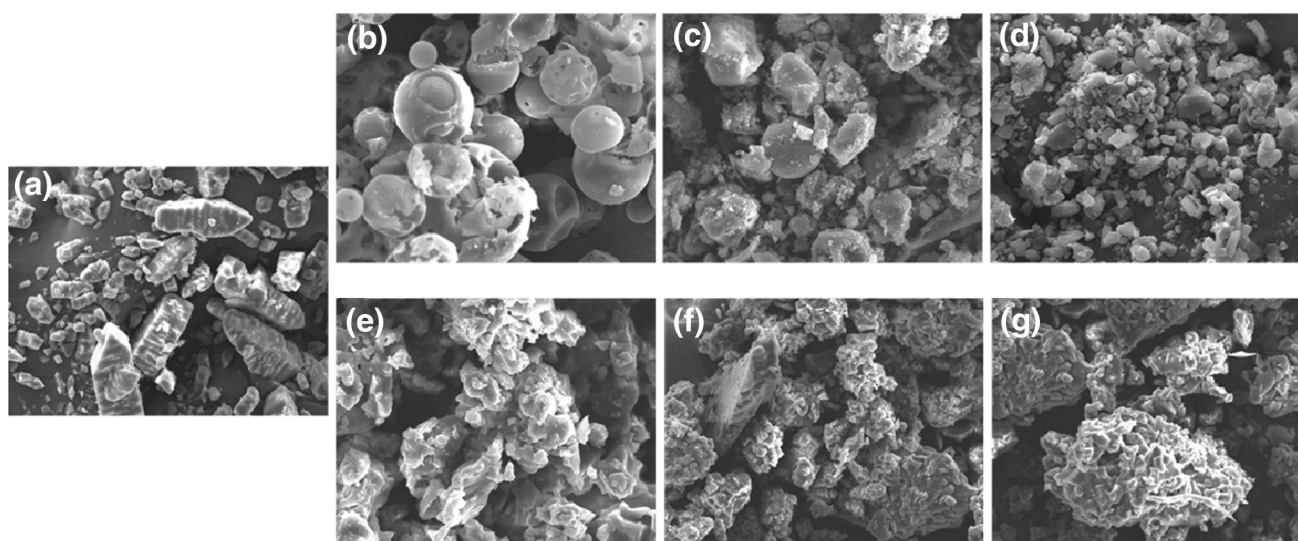
Fig. 6 SEM images of **a** AZM, **b** HP-β-CD, **c** AZM&HP-β-CD, **d** AZM-HP-β-CD, **e** HP-β-CDP, **f** AZM&HP-β-CDP, **g** AZM-HP-β-CDP (×500)
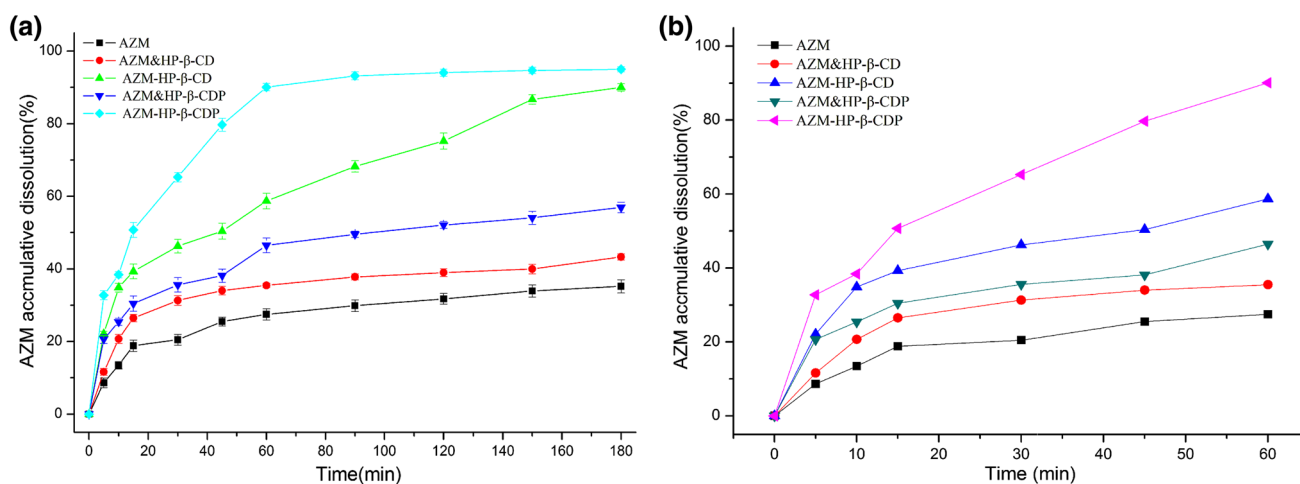

Fig. 7 The accumulative dissolution profiles of AZM, physical mixture and inclusion complexes within 180 min (**a**) and 60 min (**b**). If no *error bars* are displayed, errors were smaller than the data point size

Cumulative dissolution of AZM

The accumulative dissolution behaviors of original AZM, AZM&HP-β-CD (1:1, molar ratio), AZM&HP-β-CDP (10:1, mass ratio), AZM-HP-β-CD and AZM-HP-β-CDP were studied within 180 min. The dissolution profiles are shown in Fig. 7. The in vitro dissolution behaviors were firstly described by the time needed in which 50 % of drug was released ($T_{50 \%}$) and dissolution efficiencies (the dissolution percentage within 60 min, $D.E._{60min}$) respectively [39, 40]. $T_{50 \%}$ of AZM-HP-β-CD and AZM-HP-β-CDP was read from the dissolution profiles directly, as was over 30.6 min and over 15.8 min, while that of other samples all longer than 180 min. The analysis of $D.E._{60min}$ showed that the dissolution efficiencies towards AZM can be ranked in the following order: AZM-HP-β-CDP

(90.07 %) > AZM-HP-β-CD (58.6 %) > AZM&HP-β-CDP (46.5 %) > AZM&HP-β-CD (35.5 %) > AZM (27.5 %). Our results verified that the preparation of inclusion complex could enhance AZM dissolution compared with free drug and physical mixture as expected. The dissolution behavior of AZM-HP-β-CDP was significantly improved within 60 min in comparison to AZM-HP-β-CD, which is probably due to the many hollow polymer structures.

Discussion

Within the research field of drug delivery system, there are many formulation approaches, such as microemulsions, liposomes, nanosuspensions and prodrugs, to be widely

Table 4 Fitting results of AZM release profiles by model dependent methods

Model	Parameters	AZM	AZM&HP-β-CDP	AZM&HP-β-CDP	AZM-HP-β-CD	AZM-HP-β-CDP
a: (Within 180 min)						
First-order	K_f	−0.002	−0.002	−0.004	−0.011	−0.017
$Q_t = Q_0 \exp\left(-K_f^t\right)$	γ^2	0.799	0.697	0.829	**0.976**	0.858
Higuchi	K_H	2.49	2.83	3.80	6.25	6.89
$Q_t = K_H\sqrt{t} + C_H$	C_H	5.24	9.68	11.2	9.18	19.5
	γ^2	0.930	0.846	0.917	**0.976**	0.864
Ritger-Peppas	n	0.362	0.307	0.283	0.361	0.322
$Q_t = K_{RP}t^n$	K_{RP}	1.77	2.26	2.60	2.61	3.03
	γ^2	0.947	0.871	**0.987**	**0.980**	0.936
Weibull	k	−0.019	−0.014	−0.017	−0.017	−0.038
$M = M_0(1 - \exp(-k(t - T))$	γ^2	**0.978**	**0.910**	**0.988**	0.906	**0.986**
b: (within 60 min)						
First-order	K_f	0.005	0.006	0.008	0.012	0.035
$Q_t = Q_0 \exp\left(-K_f^t\right)$	γ^2	0.850	0.783	0.836	0.860	**0.984**
Higuchi	K_H	3.56	4.69	5.44	7.14	11.4
$Q_t = K_H\sqrt{t} + C_H$	C_H	1.49	3.21	5.43	6.16	3.45
	γ^2	**0.967**	**0.931**	0.943	**0.945**	**0.993**
Ritger-Peppas	n	0.444	0.422	0.305	0.352	0.422
$Q_t = K_{RP}t^n$	K_{RP}	1.55	1.96	2.54	2.64	2.76
	γ^2	0.946	0.896	**0.980**	0.946	**0.987**
Weibull	k	−0.021	−0.024	−0.020	−0.012	−0.044
$M_t = M_0(1 - \exp(-k(t - T))$	γ^2	0.959	0.914	0.949	**0.943**	0.961

In which M_t/Q_t is the cumulative percentage of drug dissolved as a function of time t. M_0 is total amount of drug in the preparations. T accounts for the lag time measured as a result of the dissolution process K_H, K_f, K_{RP} is the Higuchi dissolution constant; n is the release exponent; C_H is the respective intercept with the *vertical axis* of the Qt versus time curve.

Bold values indicate the best or comparable regression coefficient.

employed to improve the solubility of insoluble drugs. Of these techniques, complexation with β-CD is traditional and effective by entrapping the insoluble drugs into its nonpolar cavity. However the application of β-CD is confined by some disadvantages such as limited water solubility (18.5 mg/mL), the potential formation of crystalline complexes and so on. Since each β-CD hydroxyl group differs in its chemical reactivity, the random substitution produces an important increase in solubility due to the decrease in the crystalline state. However, increase the degree of substitution might decrease complexing capacity due to the steric hindrance of the host molecule. Numerous of β-CD derivatives by chemical modifications have been constantly developed. In which, HP-β-CD is noticeable with relatively high water solubility (500–800 mg/mL) and satisfactory inclusion ability. Many in vitro and in vivo studies also proved that the HP-β-CD inclusion complex could increase drug solubility and stability [15, 28–30, 32].

Beside the utilization of β-CD monomers, the polymers have also been developed [18, 19, 21, 25, 41]. The polymeric form can increase the stability constant of these complexes. There are mainly two kinds of macromolecular structures: polymers containing HP-β-CD pendant groups or polymers having HP-β-CD units as a part of the skeleton. The second type of polymers can be prepared by coupling the HP-β-CD with proper bifunctional agents [19, 42, 43]. The present study was designed to synthesize a more hydrophilic HP-β-CD polymer by the crosslinking of EP under the conditions of 30 % NaOH for the delivery of the poorly soluble AZM antibiotics. The reaction parameters have been verified and optimized by orthogonal design to ensure the reproducible synthesis. The chemical structure was confirmed by FT-IR and ¹H-NMR. By comparison with physical mixtures, evidence obtained by UV, FT-IR, XRD and SEM analyses demonstrated clearly that the complexation process led to the formation of a supramolecular structure in which AZM was mostly inserted into the cavity of HP-β-CD and HP-β-CDP respectively. The results of solubility studies indicated that HP-β-CDP was more efficient than parent HP-β-CD to

solubilize insoluble drug AZM by inclusion complex, which is probably due to the larger empty cavity of HP-β-CDP after polymerization.

However, due to the limited information about the complicated manners in which the drug and HP-β-CD based polymers properties interact to influence key drug delivery parameter such as dissolution. Therefore, in this study, model dependent approaches, including common empirical model (0-order, 1-order and Higuchi), semi-empirical model (Ritger-peppas, Weibull) [18, 44–47], were used to evaluate the dissolution behavior of the AZM-HP-β-CD and AZM-HP-β-CDP by the transformed linear fit method. Considering the differences of the dissolution profiles within 60 min and 180 min, the dissolution profiles were fitted separately to describe possible dissolution mechanisms. The suitability of all these models with respect to the experimental data was compared on the basis on the regression coefficient (γ^2). The fitting results are listed in Table 4. As seen from the Table 4, by the comparison of dissolution parameters, within 180 min, better fitting results could be obtained from empirical Weibull models than other models for the AZM, AZM&HP-β-CD, AZM&HP-β-CDP and AZM-HP-β-CDP groups except for AZM-HP-β-CD group. Interestingly, similar good fitting results were obtained from first-order and Ritger-Peppas model for AZM-HP-β-CD group, which suggested the solubilized AZM in HP-β-CD inclusion complex could be released in a time dependent way within 180 min. While within 60 min, Higuchi model showed some advantages for most of groups, whose mechanism was supposed to be dominated by diffusion. Unexpectedly, AZM&HP-β-CDP group was best fitted by Ritger-peppas model, in which release exponent n is used to characterize different release behavior for cylindrical shaped matrices. Also the AZM-HP-β-CD and AZM-HP-β-CDP groups obtained good fitting results in Ritger-peppas model. Thus the polymerization of HP-β-CD may be helpful to the dissolution of hydrophobic drug AZM even no direct physical interaction was observed.

Conclusions

As detailed above, we synthesized and characterized the HP-β-CDP by the polymerization of HP-β-CD under alkaline conditions. The resultant HP-β-CDP was able to solubilize AZM by the formation of inclusion complex in a more efficient way than classical HP-β-CD. The optimum preparation parameters were optimized by orthogonal design, which was molar/mass ratio (1:1 and 10:1), reaction time (3 h) and temperature (40 °C) for HP-β-CD and HP-β-CDP inclusion complex respectively. The maximum inclusion ratio of AZM-HP-β-CD and AZM-HP-β-CDP is

55.6 and 72.2 %. The results of UV–Vis, XRD and FT-IR suggested that part of lactone of AZM molecule was included into the HP-β-CD cavities from the wider edge. The solubility of AZM was significantly increased to 311.3 ± 0.26 μg/mL and 628.5 ± 0.25 μg/mL in AZM-HP-β-CD and AZM-HP-β-CDP from that of AZM 34.2 ± 0.30 μg/mL. The accumulative release profiles showed that AZM-HP-β-CDP could release over 90 % of AZM, more than AZM-HP-β-CD 60 % within 60 min. Therefore, HP-β-CDP might be a promising HP-β-CD derivative, which could broaden the design strategy of insoluble AZM delivery systems.

Compliance with ethical standards

Conflict of interest The authors herein declare there is no interest conflict.

References

1. Hu, L., Pan, J., Liu, C., Xu, H., Luo, L.: Preparation, characterization and taste-masking properties of microspheres containing azithromycin. J. Pharm. Pharmacol. **61**(12), 1631–1635 (2009). doi:10.1211/jpp/61.12.0007

2. Ishizaka, T., Okada, S., Takemoto, E., Tokuyama, E., Tsuji, E., Mukai, J., Uchida, T.: The suppression of enhanced bitterness intensity of macrolide dry syrup mixed with an acidic powder. Chem. Pharm. Bull. (Tokyo) **55**(10), 1452–1457 (2007)

3. Schmidt, L.E., Dalhoff, K.: Food-drug interactions. Drugs **62**(10), 1481–1502 (2002)

4. Bakheit, A.H., Al-Hadiya, B.M., Abd-Elgalil, A.A.: Azithromycin. Profiles Drug Subst Excip Relat Methodol **39**, 1–40 (2014). doi:10.1016/b978-0-12-800173-8.00001-5

5. Harrison, T.S., Keam, S.J.: Azithromycin extended release: a review of its use in the treatment of acute bacterial sinusitis and community-acquired pneumonia in the US. Drugs **67**(5), 773–792 (2007)

6. Uekama, K., Hirayama, F., Irie, T.: Cyclodextrin drug carrier systems. Chem. Rev. **98**(5), 2045–2076 (1998)

7. Carrier, R.L., Miller, L.A., Ahmed, I.: The utility of cyclodextrins for enhancing oral bioavailability. J. Control. Release **123**(2), 78–99 (2007). doi:10.1016/j.jconrel.2007.07.018

8. Folch-Cano, C., Yazdani-Pedram, M., Olea-Azar, C.: Inclusion and functionalization of polymers with cyclodextrins: current applications and future prospects. Molecules **19**(9), 14066–14079 (2014). doi:10.3390/molecules190914066

9. Davis, M.E., Brewster, M.E.: Cyclodextrin-based pharmaceutics: past, present and future. Nat. Rev. Drug Discov. **3**(12), 1023–1035 (2004). doi:10.1038/nrd1576

10. Dandawate, P., Vemuri, K., Khan, E.M., Sritharan, M., Padhye, S.: Synthesis, characterization and anti-tubercular activity of ferrocenyl hydrazones and their β-cyclodextrin conjugates. Carbohydr. Polym. **108**, 135–144 (2014). doi:10.1016/j.carbpol.2014.03.006

11. Szente, L., Szejtli, J.: Highly soluble cyclodextrin derivatives: chemistry, properties, and trends in development. Adv. Drug Deliv. Rev. **36**(1), 17–28 (1999)

12. García, A., Leonardi, D., Salazar, M.O., Lamas, M.C.: Modified β-cyclodextrin inclusion complex to improve the physicochemical properties of albendazole. Complete in vitro evaluation and characterization. PLoS One **9**(2), e88234 (2014). doi:10.1371/journal.pone.0088234

13. Yang, L.-J., Ma, S.-X., Zhou, S.-Y., Chen, W., Yuan, M.-W., Yin, Y.-Q., Yang, X.-D.: Preparation and characterization of inclusion complexes of naringenin with β-cyclodextrin or its derivative. Carbohydr. Polym. **98**(1), 861–869 (2013). doi:10.1016/j.carbpol.2013.07.010

14. Michel, D., Chitanda, J.M., Balogh, R., Yang, P., Singh, J., Das, U., El-Aneed, A., Dimmock, J., Verrall, R., Badea, I.: Design and evaluation of cyclodextrin-based delivery systems to incorporate poorly soluble curcumin analogs for the treatment of melanoma. Eur. J. Pharm. Biopharm. **81**(3), 548–556 (2012). doi:10.1016/j.ejpb.2012.03.016

15. Tinwalla, A.Y., Hoesterey, B.L., Xiang, T.-X., Lim, K., Anderson, B.D.: Solubilization of thiazolobenzimidazole using a combination of pH adjustment and complexation with 2-hydroxypropyl-β-cyclodextrin. Pharm. Res. **10**(8), 1136–1143 (1993). doi:10.1023/A:1018908032686

16. Zhang, Y., Ren, K., He, Z., Li, H., Chen, T., Lei, Y., Xia, S., He, G., Xie, Y., Zheng, Y., Song, X.: Development of inclusion complex of brinzolamide with hydroxypropyl-β-cyclodextrin. Carbohydr. Polym. **98**(1), 638–643 (2013). doi:10.1016/j.carbpol.2013.06.052

17. Jin, H., Liu, Y., Zheng, Y., Huang, W., Zhou, Y., Yan, D.: Cytomimetic large-scale vesicle aggregation and fusion based on host-guest interaction. Langmuir **28**(4), 2066–2072 (2012). doi:10.1021/la203857s

18. Xin, J., Guo, Z., Chen, X., Jiang, W., Li, J., Li, M.: Study of branched cationic beta-cyclodextrin polymer/indomethacin complex and its release profile from alginate hydrogel. Int. J. Pharm. **386**(1–2), 221–228 (2010). doi:10.1016/j.ijpharm.2009.11.024

19. Gidwani, B., Vyas, A.: Synthesis, characterization and application of epichlorohydrin-beta-cyclodextrin polymer. Colloids Surf. B Biointerfaces **114**, 130–137 (2014). doi:10.1016/j.colsurfb.2013.09.035

20. Renard, E., Deratani, A., Volet, G., Sebille, B.: Preparation and characterization of water soluble high molecular weight β-cyclodextrin-epichlorohydrin polymers. Eur. Polym. J. **33**(1), 49–57 (1997). doi:10.1016/S0014-3057(96)00123-1

21. Zhang, W., Gong, X., Cai, Y., Zhang, C., Yu, X., Fan, J., Diao, G.: Investigation of water-soluble inclusion complex of hypericin with beta-cyclodextrin polymer. Carbohydr. Polym. **95**(1), 366–370 (2013). doi:10.1016/j.carbpol.2013.03.020

22. Sultana, N., Arayne, M.S., Hussain, F., Fatima, A.: Degradation studies of azithromycin and its spectrophotometric determination in pharmaceutical dosage forms. Pak. J. Pharm. Sci. **19**(2), 98–103 (2006)

23. Wang, L., Li, S., Tang, P., Yan, J., Xu, K., Li, H.: Characterization and evaluation of synthetic riluzole with β-cyclodextrin and 2,6-di-O-methyl-β-cyclodextrin inclusion complexes. Carbohydr. Polym. **129**, 9–16 (2015). doi:10.1016/j.carbpol.2015.04.046

24. Ferrati, S., Nicolov, E., Bansal, S., Hosali, S., Landis, M., Grattoni, A.: Docetaxel/2-Hydroxypropyl β-cyclodextrin Inclusion complex increases docetaxel solubility and release from a nanochannel drug delivery system. Curr. Drug Targets **16**(14), 1645–1649 (2015)

25. Auda, S.H.: Nimesulide/methyl β-cyclodextrin inclusion complexes: physicochemical characterization, solubility, dissolution,

and biological studies. Drug Dev. Res. **75**(2), 68–75 (2014). doi:10.1002/ddr.21156

26. Ai, F., Ma, Y., Wang, J., Li, Y.: Preparation, physicochemical characterization and in-vitro dissolution studies of diosmin-cyclodextrin inclusion complexes. Iran. J. Pharm. Res : IJPR **13**(4), 1115–1123 (2014)

27. Patel, J.S., Patel, R.P.: Preparation, characterization and in vitro dissolution study of Nitrazepam: cyclodextrin inclusion complex. J. Pharm. Bioallied Sci. **4**(Suppl 1), S106–S107 (2012). doi:10.4103/0975-7406.94158

28. Glisoni, R.J., Cuestas, M.L., Mathet, V.L., Oubiña, J.R., Moglioni, A.G., Sosnik, A.: Antiviral activity against the hepatitis C virus (HCV) of 1-indanone thiosemicarbazones and their inclusion complexes with hydroxypropyl-β-cyclodextrin. Eur. J. Pharm. Sci. **47**(3), 596–603 (2012). doi:10.1016/j.ejps.2012.07.018

29. Qiu, N., Cheng, X., Wang, G., Wang, W., Wen, J., Zhang, Y., Song, H., Ma, L., Wei, Y., Peng, A., Chen, L.: Inclusion complex of barbigerone with hydroxypropyl-β-cyclodextrin: preparation and in vitro evaluation. Carbohydr. Polym. **101**, 623–630 (2014). doi:10.1016/j.carbpol.2013.09.035

30. de Araujo, D.R., Tsuneda, S.S., Cereda, C.M., Carvalho, F.D.G., Prete, P.S., Fernandes, S.A., Yokaichiya, F., Franco, M.K., Mazzaro, I., Fraceto, L.F., de FA Braga, A., de Paula, E.: Development and pharmacological evaluation of ropivacaine-2-hydroxypropyl-beta-cyclodextrin inclusion complex. Eur J Pharm Sci **33**(1), 60–71 (2008). doi:10.1016/j.ejps.2007.09.010

31. Hu, L., Zhang, H., Song, W., Gu, D., Hu, Q.: Investigation of inclusion complex of cilnidipine with hydroxypropyl-β-cyclodextrin. Carbohydr. Polym. **90**(4), 1719–1724 (2012). doi:10.1016/j.carbpol.2012.07.057

32. Yao, Y., Xie, Y., Hong, C., Li, G., Shen, H., Ji, G.: Development of a myricetin/hydroxypropyl-β-cyclodextrin inclusion complex: preparation, characterization, and evaluation. Carbohydr. Polym. **110**, 329–337 (2014). doi:10.1016/j.carbpol.2014.04.006

33. Miro, A., Ungaro, F., Balzano, F., Masi, S., Musto, P., La Manna, P., et al.: Triamcinolone solubilization by (2-hydroxypropyl)-beta-cyclodextrin: a spectroscopic and computational approach. Carbohydr. Polym. **90**(3), 1288–1298 (2012)

34. Jiang, H., Zhang, S., Guan, Q., Chen, C., Gao, F., Zhang, Y.: 1H NMR investigations of inclusion complexes between beta-cyclodextrin and 1-hexadecanol. Curr. Drug Discov. Technol. **4**(4), 295–297 (2007)

35. Li, Z., Xu, H., Li, S., Li, Q., Zhang, W., Ye, T., Yang, X., Pan, W.: A novel gastro-floating multiparticulate system for dipyridamole (DIP) based on a porous and low-density matrix core: in vitro and in vivo evaluation. Int. J. Pharm. **461**(1–2), 540–548 (2014). doi:10.1016/j.ijpharm.2013.12.024

36. Lin, J., Wang, X., Wu, Q., Dai, J., Guan, H., Cao, W., He, L., Wang, Y.: Development of Salvianolic acid B-Tanshinone II A-Glycyrrhetinic acid compound liposomes: formulation optimization and its effects on proliferation of hepatic stellate cells. Int. J. Pharm. **462**(1–2), 11–18 (2014). doi:10.1016/j.ijpharm.2013.12.040

37. Srinivasan, K., Sivakumar, K., Stalin, T.: 2,6-Dinitroaniline and β-cyclodextrin inclusion complex properties studied by different analytical methods. Carbohydr. Polym. **113**, 577–587 (2014). doi:10.1016/j.carbpol.2014.07.062

38. Rajendiran, N., Siva, S.: Inclusion complex of sulfadimethoxine with cyclodextrins: preparation and characterization. Carbohydr. Polym. **101**, 828–836 (2014). doi:10.1016/j.carbpol.2013.10.016

39. Gidwani, B., Vyas, A.: Inclusion complexes of bendamustine with beta-CD: HP-beta-CD and Epi-beta-CD: in vitro and in vivo evaluation. Drug Dev. Ind. Pharm. (2015). doi:10.3109/03639045.2015.1027217

40. de Freitas, M.R., Rolim, L.A., Soares, M.F.D.L.R., Rolim-Neto, P.J., de Albuquerque, M.M., Soares-Sobrinho, J.L.: Inclusion complex of methyl-β-cyclodextrin and olanzapine as potential drug delivery system for schizophrenia. Carbohydr. Polym. **89**(4), 1095–1100 (2012). doi:10.1016/j.carbpol.2012.03.072

41. Qian, L., Guan, Y., Xiao, H.: Preparation and characterization of inclusion complexes of a cationic beta-cyclodextrin polymer with butylparaben or triclosan. Int. J. Pharm. **357**(1–2), 244–251 (2008). doi:10.1016/j.ijpharm.2008.01.018

42. Jeon, W.B., Bae, K.H., Byun, S.M.: Dimeric beta-cyclodextrin-based supramolecular ligands and their copper(II) complexes as metalloenzyme models. J. Inorg. Biochem. **71**(3–4), 163–169 (1998)

43. Lu, X., Ping, Y., Xu, F.J., Li, Z.H., Wang, Q.Q., Chen, J.H., Yang, W.T., Tang, G.P.: Bifunctional conjugates comprising beta-cyclodextrin, polyethylenimine, and 5-fluoro-2'- deoxyuridine for drug delivery and gene transfer. Bioconjug Chem. **21**(10), 1855–1863 (2010). doi:10.1021/bc1002136

44. Yang, R., Chen, J.-B., Xiao, C.-F., Liu, Z.-C., Gao, Z.-Y., Yan, S.-J., Zhang, J.-H., Zhang, H.-B., Lin, J.: Inclusion complex of GA-13316 with β-cyclodextrin: preparation, characterization, molecular modeling, and in vitro evaluation. Carbohydr. Polym. **111**, 655–662 (2014). doi:10.1016/j.carbpol.2014.05.021

45. Ghosal, K., Chandra, A., Rajabalaya, R., Chakraborty, S., Nanda, A.: Mathematical modeling of drug release profiles for modified hydrophobic HPMC based gels. Pharmazie **67**(2), 147–155 (2012)

46. Jacobsen, J., Bjerregaard, S., Pedersen, M.: Cyclodextrin inclusion complexes of antimycotics intended to act in the oral cavity—drug supersaturation, toxicity on TR146 cells and release from a delivery system. Eur. J. Pharm. Biopharm. **48**(3), 217–224 (1999). doi:10.1016/S0939-6411(99)00043-0

47. Tan, Q., Li, Y., Wu, J., Mei, H., Zhao, C., Zhang, J.: An optimized molecular inclusion complex of diferuloylmethane: enhanced physical properties and biological activity. Int. J. Nanomed. **5**, 5385–5393 (2012). doi:10.2147/ijn.s36404